

# Structural properties and quasiparticle energies of cubic SrO, MgO and SrTiO<sub>3</sub>

Giancarlo Cappellini

*INFM Sezione di Cagliari and Dipartimento di Fisica, Università di Cagliari, Cittadella Universitaria, Strada Provinciale Monserrato-Sestu km.0.700, I-09042 Monserrato (Ca), Italy*

Sophie Bouette-Russo, Bernard Amadon, Claudine Noguera and Fabio Finocchi

*Laboratoire de Physique des Solides, UMR CNRS 8502, Bâtiment 510, Université Paris-Sud, 91405 Orsay, France*

The structural properties and the band structures of the charge-transfer insulating oxides SrO, MgO and SrTiO<sub>3</sub> are computed both within density functional theory in the local density approximation (LDA) and in the Hedin's GW scheme for self-energy corrections, by using a model dielectric function, which approximately includes local field and dynamical effects. The deep valence states are shifted to higher binding energies by the GW method, in very good agreement with photoemission spectra. Since in all these oxides the direct gaps at high-symmetry points of the Brillouin zone may be strongly sensitive to the actual value of the lattice parameter  $a$ , already at the LDA level, self-energy corrections are computed both at the theoretical and the experimental  $a$ . For MgO and SrO, the values of the transition energies between the valence and the conduction bands is improved by GW corrections, while for SrTiO<sub>3</sub> they are overestimated. The results are discussed in relation to the importance of local field effects and to the nature of the electronic states in these insulating oxides.

## I. INTRODUCTION

Aside from being the major constituent of the outer crust of the earth, oxides are of considerable interest for their wide applications in various technological fields such as electrochemistry, catalysis or microelectronics.<sup>1</sup> They present very diverse electronic ground states which range from superconducting, metallic, semi-conducting (intrinsic, charge density- or spin density-like) to insulating. From a theoretical point of view, a proper description of their electronic properties is still an active research subject. On the one hand, several transition metal oxides require an inclusion of many-body effects beyond the available effective one-electron approaches, such as the density functional theory (DFT) or the *ab initio* Hartree-Fock (HF) method. On the other hand, even for insulating charge transfer oxides, such as MgO and SrO, whose electronic ground state is well accounted for in a one-electron picture, the calculation of quasiparticle (QP) energies within the DFT or the HF method gives rather poor results. Indeed, one has to face the so-called energy band gap problem<sup>2</sup>. Indeed, when using the Kohn-Sham eigenvalues of the highest occupied and the lowest empty states, the resulting gap usually underestimates the experimental data. On the other hand, the corresponding difference between the HF eigenvalues overestimates the gap severely. Alternative ways to calculate the band gap in infinite systems have been found, in the framework of HF or DFT. One of them is based on total energy differences between ground and charge transfer states<sup>3</sup>. The other one relies on the value of the gap found in the one electron spectrum of the ionized or hole-doped system<sup>4</sup>. However, such methods are unable to provide the full QP spectrum.

In the last decade, due to the implementation of angular resolved photoemission experiments able to cope with charging effects on insulating oxides, detailed QP spectra of MgO<sup>5</sup>, SrTiO<sub>3</sub><sup>6</sup> or TiO<sub>2</sub><sup>7,8</sup> among other oxides, have become available. The experimental achievements demand systematic improvements in the theoretical description of the electronic excitations of simple oxides.

In semiconducting and ionic crystalline compounds, corrections to the DFT eigenvalues, as obtained from the Kohn-Sham equations, may be estimated by first-order many-body perturbation theory<sup>9-11</sup>, with respect to the difference between the exchange-correlation (XC) self-energy and the corresponding XC potential of the DFT, for which various approximations are available. Within the same approach, the self-energy operator is treated in the GW approximation proposed by Hedin<sup>9</sup>. Such calculations have been carried out with success in several semiconducting and insulating crystals<sup>10-15</sup>, permitting the prediction of the quasiparticle energies and the calculation of optical properties of real solids.

One of the crucial points in such calculations is the evaluation of the self-energy operator, which is numerically very expensive, because of the required knowledge of the full inverse dielectric matrix of the system under study. This is a bottleneck for the application of the method to systems with a large number of atoms in the unit cell, such as surfaces<sup>16,17</sup> and defective or low-symmetry solids. In order to reduce the remarkable numerical effort and be able to predict electronic excited states in a wider range of real systems, one may use efficient GW methods, in which a model dielectric function is used to mimic the screening properties of the system under study.

Pioneering work in this direction has been performed by Bechstedt and Del Sole in a tight-binding scheme<sup>18</sup> and by Gygi and Baldereschi<sup>19</sup> within the DFT in the Local Density Approximation (LDA) for the exchange and correlation energy. The key of their work relies (*i*) on the use of a model dielectric function, which mimics the main screening properties of semiconductors, and (*ii*) on an approximated self-energy operator in which both local fields and dynamical screening – giving rise to opposite contributions to band gaps – are neglected.<sup>10,18,19</sup> For a large family of semiconductors, the band gaps obtained through these simplified methods show good accordance both with experiments and full GW results, in which the screening properties of the system are calculated from first principles. More recently, an efficient GW method that approximately includes dynamical-screening and local field effects, without increasing the computational effort, has been formulated<sup>20</sup> and proved to reproduce quasiparticle energies and band gaps for either bulk zincblende solids (ranging from Si, GaAs, AlAs to the more ionic ZnSe)<sup>21</sup> or non cubic systems (BN<sup>22</sup>, SiC polytypes<sup>23,24</sup>) satisfactorily. The method is based on a linear expansion of the dynamical contribution to the exchange-correlation self-energy, on the use of a model dielectric function, and on a local ansatz for the treatment of the intrinsically non local screened interaction. Depending on the system, the speedup of the calculation may result of two order of magnitude with respect to corresponding full GW ones. Moreover, this kind of GW calculations is feasible on a standard workstation.

The aim of the present paper is to study the ground state properties of cubic magnesium oxide, strontium oxide and strontium titanate, in the DFT-LDA scheme, as well as their quasiparticle band structures within the efficient GW scheme. On one hand, no previous GW calculation of SrO or SrTiO<sub>3</sub> exists, to our knowledge. On the other hand, these charge transfer oxides are characterized by different fundamental gaps, ranging from  $\simeq 3$  eV (SrTiO<sub>3</sub>) to  $\simeq 7.7$  eV (MgO), as given by experimental data. Their bandstructures may substantially differ from those of the semiconductors cited above, due to the presence of strongly localized electronic states. Thus, such a study may also represent a test for the approximate GW scheme, originally proposed for small-gap semiconductors, to show its

capabilities relatively to a different class of physical systems.

The paper is organized as follows. The theoretical framework is depicted in Section II and it is followed, in Section III, by a description of the computational ingredients used for the description of structural and electronic properties of MgO, SrO and SrTiO<sub>3</sub>. The results obtained for these systems are presented separately in Sections IV, V and VI, respectively. Finally, in Section VII we present our conclusions and the perspectives opened by our work.

## II. GW CORRECTIONS

The energy  $E_{n\vec{k}}$  of a quasiparticle in a band  $n$  at a given  $\vec{k}$  point in the Brillouin zone can be obtained through the equation:<sup>10,25,11</sup>

$$\left[ -\frac{\nabla^2}{2} + V_{\text{ext}}(\vec{r}) + V_{\text{H}}(\vec{r}) \right] \phi_{n\vec{k}}(\vec{r}) + \int d^3\vec{r}' \Sigma(\vec{r}, \vec{r}'; E_{n\vec{k}}) \phi_{n\vec{k}}(\vec{r}') = E_{n\vec{k}} \phi_{n\vec{k}}(\vec{r}) \quad (1)$$

which is written in atomic units ( $e=\hbar=m_e=1$ ).  $V_{\text{ext}}(\vec{r})$  is the external potential originated by the ions,  $V_{\text{H}}(\vec{r})$  is the Hartree potential and  $\Sigma$  is the mass operator, usually called the self-energy operator, which is in general non local, non-Hermitian and energy dependent. In principle it contains the exchange and correlation effects and is state ( $n\vec{k}$ ) dependent. One can compare the above equation to that of Kohn and Sham<sup>26</sup>:

$$\left[ -\frac{\nabla^2}{2} + V_{\text{ext}}(\vec{r}) + V_{\text{H}}(\vec{r}) + V_{\text{xc}}(\vec{r}) \right] \psi_{n\vec{k}}(\vec{r}) = E_{n\vec{k}}^{(0)} \psi_{n\vec{k}}(\vec{r}) \quad (2)$$

where  $V_{\text{xc}}$  is the exchange–correlation potential of the DFT (for which several approximation are available), and the superscript <sup>(0)</sup> will denote the quantities computed at the DFT level from now on.  $E_{n\vec{k}}^{(0)}$  is usually considered as a first approximation to the quasiparticle energy. The failure of this scheme for evaluating transition energies  $E_{n'\vec{k}} - E_{n\vec{k}}$  between different quasiparticle states in solids has been evidenced by many authors<sup>2,10,11</sup>.

One can correct the DFT eigenvalues  $E_{n\vec{k}}^{(0)}$ , in a first-order perturbation theory with respect to  $\Sigma_{n\vec{k}} - V_{\text{xc}}$ , and estimate the QP energies as:

$$E_{n\vec{k}} \simeq E_{n\vec{k}}^{(0)} + \langle \psi_{n\vec{k}} | \Sigma(\vec{r}, \vec{r}'; E_{n\vec{k}}) - V_{\text{xc}}(\vec{r}) | \psi_{n\vec{k}} \rangle \quad (3)$$

The evaluation of  $\Sigma(\vec{r}, \vec{r}'; E_{n\vec{k}})$  is in general a very difficult task. A possible approximation is the GW one,<sup>9</sup> in which a perturbation expansion for the self-energy can be constructed and stopped at the first order:

$$\Sigma(\vec{r}, \vec{r}'; \omega) = i \int_{-\infty}^{+\infty} \frac{d\omega'}{2\pi} e^{i\delta\omega'} G(\vec{r}, \vec{r}'; \omega + \omega') W(\vec{r}, \vec{r}'; \omega') \quad (4)$$

where  $G$  is the one-particle Green function,  $W$  is the screened Coulomb interaction and  $\delta = 0^+$ . Following Bechstedt and coworkers,<sup>2,20</sup> the real part of the self-energy operator (which is relevant for the corrections to the QP bandstructure) may be separated in a dynamic and a static contribution, and written as:

$$\Re \Sigma(\vec{r}, \vec{r}'; \omega) = \Sigma^{\text{sex}}(\vec{r}, \vec{r}') + \Sigma^{\text{coh}}(\vec{r}, \vec{r}') + \Sigma^{\text{dyn}}(\vec{r}, \vec{r}'; \omega) \quad (5)$$

$\Sigma^{\text{sex}}$  and  $\Sigma^{\text{coh}}$  are the static screened–exchange (SEX) and the coulomb–hole (COH) terms, respectively, and  $\Sigma^{\text{dyn}}$  the energy dependent contribution. Although the previous equation is purely formal, it is the starting point of simplified GW schemes, since one can work out approximated expressions for each contribution separately. The most expensive step towards the evaluation of GW corrections to  $E_{n\vec{k}}^{(0)}$  is the calculation of the energy-dependent screened interaction  $W(\vec{r}, \vec{r}'; \omega)$ . Although many improvements have been proposed for an efficient calculation of the dielectric response function from first principles,<sup>27,28</sup> still this stage is both computer time and memory very demanding when a large basis set is used for the description of the electronic structure. In particular, this is the case of oxides in a plane-wave pseudopotential approach. On the other hand, the improvement of DFT–LDA band structures obtained by using schemes originally formulated on phenomenological basis, such as the scissor operator or the Slater’s  $\alpha$  potential,<sup>2</sup> showed that the essential physics can be described through the use of effective or state-dependent potentials. From a more fundamental point of view, one can work out a model for the screening properties of the system, and look to what extent the computed QP spectra account for the observed experimental values. Possibly, the model should also be simple enough to be generalized to a large number of different systems. Following previous studies,<sup>20,23</sup> we use a model dielectric function to estimate both the static and the dynamical contributions to the self-energy (Eq.5), since it is the key ingredient entering the efficient GW approximations.

## A. Static Screening and Local Field Effects

For the diagonal part of the screening function, we use an analytical model originally proposed by Bechstedt and Del Sole:<sup>18</sup>

$$\epsilon(q, \bar{\rho}) = 1 + \left[ \frac{1}{\epsilon_\infty - 1} + \frac{q^2}{q_{TF}^2} + \frac{3q^4}{4k_F^2 q_{TF}^2} \right]^{-1} \quad (6)$$

where the Fermi vector  $k_F$  and the Thomas-Fermi wave-vector  $q_{TF}$  depend on the average electron density  $\bar{\rho}$ . This expression mimics the free electron gas behavior at high  $q$ . At  $q = 0$ , Eq.6 gives the value of the optical dielectric constant  $\epsilon_\infty$  of the oxide. Moreover we use a local *ansatz* for the static Coulomb screened interaction, analogously to that of Hybertsen and Louie<sup>27</sup>:

$$W(\vec{r}, \vec{r}') = \frac{1}{2} [W^h(\vec{r} - \vec{r}'; \rho(\vec{r})) + W^h(\vec{r} - \vec{r}'; \rho(\vec{r}'))] \quad (7)$$

where  $W^h$  is the screened Coulomb interaction of a virtual homogeneous system characterized by a finite optical dielectric constant.<sup>18,29</sup> Quasiparticle energies determined from the above *ansatz* result in good accordance with full GW calculated ones.<sup>20,27</sup> It permits, together with Eq.(6), to obtain a simple analytical expression for the static part of the Coulomb hole self energy  $\Sigma^{\text{coh}}$ . The explicit formula has been given elsewhere.<sup>30</sup> For the calculation of  $\Sigma^{\text{sex}}$  in Eq.5, the Fourier transform of  $W(\vec{r}, \vec{r}')$  is needed, namely  $\tilde{W}(\vec{k} + \vec{G}, \vec{k} + \vec{G}')$ . In order to reduce sharply the time needed to compute this term, we proceed in two steps. Firstly, we retain only the diagonal terms in the screened coulomb interaction. Secondly, we account for local field effects (*i.e.* non diagonal terms with  $\vec{G} \neq \vec{G}'$  in  $\tilde{W}$ ) by using suitable state-dependent densities to compute  $k_F$  and  $q_{TF}$ . Given a state  $n\vec{k}$ , we define the effective electron density  $\tilde{\rho}_{n\vec{k}}$ , which determines the typical screening lengths  $q_{TF}^{-1}$  and  $k_F^{-1}$ , relevant for the estimation of  $E_{n,\vec{k}}$  (Eq.3) as the expectation value of the ground state electronic density  $\rho(\vec{r})$  on the actual state:

$$\tilde{\rho}_{n\vec{k}} = \int d^3\vec{r} \rho(\vec{r}) |\psi_{n\vec{k}}(\vec{r})|^2. \quad (8)$$

Since the relevant screening lengths  $k_F^{-1}$  and  $q_{TF}^{-1}$  are increasing functions of  $\tilde{\rho}_{n\vec{k}}$ , the latter is intended to give an approximate description of the local fields in  $\Sigma^{\text{sex}}$  through an enhanced screening for the electronic states which contribute effectively to the total electron density. In the oxides considered here, the effective densities  $\tilde{\rho}_{n\vec{k}}$  range from few tenths of the mean valence electron density  $\bar{\rho} = Z_{\text{val}}/V$  for conduction states up to 4–5  $\bar{\rho}$  for deep valence states. As a consequence, the lengths  $k_F^{-1}$  and  $q_{TF}^{-1}$  are shorter for the screening of valence band states than for conduction band states. This difference is enhanced with respect to more covalent semiconductors, such as Si and GaAs<sup>20</sup>, in which the valence electron distribution is more delocalized and less dissimilar from that of the conduction states than in oxides such as MgO.

This approximate scheme for treating local field effects was analyzed in detail and its reliability was shown through a comparison with full GW calculations, in the case of both small- and wide-gap semiconductors<sup>20,21</sup>. In Ref. 21, it was also shown that the use of a non-diagonal model dielectric function does not clearly improve band gaps while bringing additional computational costs.

## B. Dynamical contributions

The diagonal matrix element of the dynamical part of the self energy (the third operator on the right side in Eq.5) on the state  $\psi_{n\vec{k}}$ :

$$\Sigma_{n\vec{k}}^{\text{dyn}}(\omega) = \langle \psi_{n\vec{k}} | \Sigma^{\text{dyn}}(\vec{r}, \vec{r}'; \omega) | \psi_{n\vec{k}} \rangle \quad (9)$$

can be linearly expanded in energy around the DFT value  $E_{n\vec{k}}^{(0)}$ , with linear coefficient:

$$\beta_{n\vec{k}} = \langle \psi_{n\vec{k}} | \left( \frac{\partial \Sigma}{\partial \omega} \right)_{E_{n\vec{k}}^{(0)}} | \psi_{n\vec{k}} \rangle. \quad (10)$$

This approximation for the energy dependence of the self-energy operator turns out to be valid in a wide energy range, as confirmed by the results of full GW calculations on bulk Si.<sup>10</sup> Solving the Dyson equation within the first-order perturbation theory with respect to  $\Sigma - V_{\text{xc}}$ , and using Eqs.3 and 5, the QP shifts for the  $\psi_{n\vec{k}}$  state hence read:

$$E_{n\vec{k}} - E_{n\vec{k}}^{(0)} = \frac{\Sigma_{n\vec{k}}^{\text{coh}} + \Sigma_{n\vec{k}}^{\text{sex}} + \Sigma_{n\vec{k}}^{\text{dyn}}(E_{n\vec{k}}^{(0)}) - \langle \psi_{n\vec{k}} | V_{\text{xc}} | \psi_{n\vec{k}} \rangle}{1 + \beta_{n\vec{k}}}, \quad (11)$$

where  $\Sigma_{n\vec{k}}^{\text{coh}}$  and  $\Sigma_{n\vec{k}}^{\text{sex}}$  are the expectation values of the static COH and SEX contributions to the self energy, respectively. From the GW expression of  $\Sigma$ , replacing G by  $G^{(0)}$ , computed at the DFT level<sup>20</sup> :

$$\Sigma_{n\vec{k}}^{\text{dyn}}(E_{n\vec{k}}^{(0)}) = \sum_{n'\vec{k}'} \int \frac{d^3 \vec{q}}{(2\pi)^3} |B_{nn'}^{\vec{k}\vec{k}'}(\vec{q})|^2 \frac{4\pi}{q^2} (E_{n\vec{k}}^{(0)} - E_{n'\vec{k}'}^{(0)}) P \int_0^\infty \frac{d\omega}{\omega\pi} \frac{\Im(\epsilon^{-1}(\vec{q}, \tilde{\rho}_{n\vec{k}}, \omega))}{\omega - \text{sgn}(E_{n'\vec{k}'}^{(0)} - \mu)(E_{n\vec{k}}^{(0)} - E_{n'\vec{k}'}^{(0)})} \quad (12)$$

$$\beta_{n\vec{k}} = \sum_{n'\vec{k}'} \int \frac{d^3 \vec{q}}{(2\pi)^3} |B_{nn'}^{\vec{k}\vec{k}'}(\vec{q})|^2 \frac{4\pi}{q^2} P \int_0^\infty \frac{d\omega}{\pi} \frac{\Im(\epsilon^{-1}(\vec{q}, \tilde{\rho}_{n\vec{k}}, \omega))}{\left[\omega - \text{sgn}(E_{n'\vec{k}'}^{(0)} - \mu)(E_{n\vec{k}}^{(0)} - E_{n'\vec{k}'}^{(0)})\right]^2} \quad (13)$$

where

$$B_{nn'}^{\vec{k}\vec{k}'}(\vec{q}) = \int d^3 \vec{r} \psi_{n\vec{k}}^*(\vec{r}) e^{i\vec{q}\cdot\vec{r}} \psi_{n'\vec{k}'}(\vec{r}) \quad (14)$$

The model  $\epsilon^{-1}$  is diagonal in  $q$  space and the local field effects are accounted for through the use of the state averaged density  $\tilde{\rho}_{n\vec{k}}$  (Eq.8). The  $\omega$ -dependent dielectric function is obtained from the static one by means of the plasmon-pole approximation (PPA)<sup>10</sup>. The PPA has been widely used to compute semiconductor and insulator quasiparticle bandstructures, even in the energy range of semicore states<sup>12–14</sup>. In order to account for the differences  $E_{n\vec{k}}^{(0)} - E_{n'\vec{k}'}^{(0)}$  in Eqs.12 and 13, replacing them with the state independent form  $E_{n\vec{k}}^{(0)} - E_{n'\vec{k}'}^{(0)} \approx -q^2/2$  as in Ref. 20, and using the sum rule  $\sum_{n'\vec{k}'} |B_{nn'}^{\vec{k}\vec{k}'}(\vec{q})|^2 = 1$ , one obtains:

$$\Sigma_{n\vec{k}}^{\text{dyn}}(E_{n\vec{k}}^{(0)}) \simeq \int \frac{d^3 \vec{q}}{(2\pi)^3} P \int_0^\infty \frac{d\omega}{\omega\pi} \frac{\Im(\epsilon^{-1}(\vec{q}, \tilde{\rho}_{n\vec{k}}, \omega))}{\omega + \frac{q^2}{2}} \quad (15)$$

$$\beta_{n\vec{k}} \simeq \int \frac{d^3 \vec{q}}{(2\pi)^3} \frac{4\pi e^2}{q^2} P \int_0^\infty \frac{d\omega}{\pi} \frac{\Im(\epsilon^{-1}(\vec{q}, \tilde{\rho}_{n\vec{k}}, \omega))}{(\omega + \frac{q^2}{2})^2} \quad (16)$$

Therefore, once the spectrum and eigenfunctions obtained in the framework of the DFT are known, the calculation of  $\Sigma_{n\vec{k}}^{\text{dyn}}(E_{n\vec{k}}^{(0)})$  and  $\beta_{n\vec{k}}$  according to Eqs.15 and 16 needs no additional external parameters apart from the model dielectric function, and results a simple task that can be carried out on a standard workstation.

We have made extensive checks to test the reliability of the approximations used to obtain Eqs.15 and 16, in the case of Silicon. Some transitions between high-symmetry points of some valence and conduction band states in Si are compared in Tables I to those obtained through full GW. The energy of the transitions between high-symmetry points, as well as the fundamental gap in Si, are in very close agreement with those obtained from full GW calculations and with experiments for both methods. As far as the QP eigenvalues in Si are concerned, the top of the valence band  $\Gamma_{25',v}$  is shifted downwards with respect to the DFT values of 0.28 eV. This can be compared with the upward shift of 0.07 eV, as found by Godby *et al.*<sup>11</sup>.

Si	full GW <sup>(a)</sup>	full GW <sup>(b)</sup>	this work	Exp.
$\Gamma_{1,v} - \Gamma_{25',v}$	12.04		12.09	$12.5 \pm 0.6$
$\Gamma_{25',v} - \Gamma_{15,c}$	3.35	3.30	3.33	3.4
$\Gamma_{25',v} - \Gamma_{2',c}$	4.08	4.27	4.25	4.2
$L_{2',v} - \Gamma_{25',v}$	9.79		9.98	$9.3 \pm 0.4$
$L_{1,v} - \Gamma_{25',v}$	7.18		7.27	$6.7 \pm 0.2$
$L_{3',v} - \Gamma_{25',v}$	1.27		1.25	$1.2 \pm 0.2, 1.5$
$\Gamma_{25',v} - L_{1,c}$	2.27	2.30	2.22	$2.4 \pm 0.2, 2.1$
$\Gamma_{25',v} - L_{3,c}$	4.24	4.11	4.15	$4.15 \pm 0.1$
$L_{3',v} - L_{1,c}$	3.54		3.47	3.45
$L_{3',v} - L_{3,c}$	5.51		5.41	5.50
$X_{4,v} - \Gamma_{25',v}$	2.99		2.98	$3.3 \pm 0.2, 2.9$

$\Gamma_{25',v} - X_{1,c}$	1.44	1.24	1.54	1.3
$v - c$ minimal gap	1.29		1.21	1.17

TABLE I. Computed vertical transitions and minimal valence–conduction band gap for Silicon (in eV). (a): Ref. 27. (b): Ref. 11. The experimental values are quoted in Ref. 27.

### III. COMPUTATIONAL DETAILS

The Density Functional calculations are carried out within the LDA for exchange and correlation<sup>31</sup>. The Kohn–Sham orbitals are expanded in a plane–wave basis set. Special care has been used in constructing the pseudopotentials for cations (Sr, Ti, Mg), in order to avoid the occurrence of ghost states<sup>32</sup> and to assure an optimal transferability over a wide energy range. We find that the inclusion of semicore states, such as 4s and 4p states for Sr, and 3s and 3p states for Ti, greatly improves the transferability of the pseudopotentials, and is at the same time necessary to take into account the hybridization of cation semicore states with O 2s states.

Angular components up to  $l = 2$  are included. The scheme of Martins and Troullier is used<sup>33</sup> to generate separable soft norm–conserving pseudopotentials, with core radii (bohr): 2.00 (Sr, 4s), 1.50 (Sr, 4p), 1.90 (Sr, 4d); 1.30 (Ti, 3s), 1.40 (Ti, 3p), 1.80 (Ti, 3d); 1.38 (O, 2s), 1.60 (O, 2p), 1.38 (O, 3d); 2.00 (Mg, 3s, 3p, 3d). The cutoff energy needed to obtain a convergence better than 0.1 eV of both total energy and Kohn–Sham eigenvalues is found to be equal to 50 Ry for MgO, 60 Ry for SrO and 80 Ry for SrTiO<sub>3</sub>.

The use of 10 special  $\vec{k}$  points<sup>34</sup> for charge integration in the irreducible wedge of the Brillouin Zone (IBZ) is sufficient to achieve a good accuracy for the computed total energy; for instance, the total energy changes by less than 10 meV and the fundamental band gap by less than 0.1 eV when using 10 instead of 6 special points to sample the IBZ.

The main bottleneck in the ab–initio GW calculations is the calculation and the inversion of the full dielectric matrix from the eigenfunctions and eigenvalues of the system. Typically, this task takes approximatively 75% of CPU time needed for the calculation of the self–energy correction for a single state<sup>2</sup>. As a result of the use of a model screening, the computational cost and memory requirement are strongly reduced, and are comparable to those of calculations carried out within the DFT. Efficient GW calculations can thus be carried out also on a common workstation.<sup>35</sup>

The evaluation of the GW corrections to the LDA bandstructures, and especially of the SEX contribution  $\Sigma^{\text{sex}}$  to the self–energy, needs some care, due to the presence of an integrable divergence. A reduction of the numerical effort by using a limited number of  $k$  points in the IBZ is possible through the method proposed by Gygi and Baldereschi<sup>36</sup>. In our calculations, the regularization is performed, for all the  $\vec{k}$ –points for which  $\Sigma^{\text{sex}}$  is calculated, by transforming the integral over the BZ of the diverging contribution into an integral of a function  $F(\vec{k})$  (periodic over the BZ), that can be computed analytically, plus a discrete sum over special  $\vec{k}$ –points of a smooth function. For the sake of conciseness, in the case of the bare exchange term (the generalization to the case of the diagonal screened exchange in cubic systems is straightforward), the transformation reads:

$$\Omega \int_{BZ} \frac{d^3 k'}{(2\pi)^3} \frac{|B_{nn'}^{\vec{k}\vec{k}'}(\vec{g})|^2}{|\vec{k}' - \vec{k} - \vec{g}|^2} \simeq \Omega \int_{BZ} \frac{d^3 k'}{(2\pi)^3} F(\vec{k}') |B_{nn'}^{\vec{k}\vec{k}'}(0)|^2 + \sum_{\vec{k}'} w_{\vec{k}'} \left[ \frac{|B_{nn'}^{\vec{k}\vec{k}'}(\vec{g})|^2}{|\vec{k}' - \vec{k} - \vec{g}|^2} - \theta^{\text{BZ}}(\vec{k}' - \vec{k} - \vec{g}) |B_{nn'}^{\vec{k}\vec{k}'}(0)|^2 F(\vec{k}' - \vec{k}) \right]. \quad (17)$$

$\theta^{\text{BZ}}(\vec{q}) = 1$  if  $\vec{q} \in \text{BZ}$  and zero otherwise,  $B_{nn'}^{\vec{k}\vec{k}'}(\vec{g})$  has previously been defined (Eq.14), and  $w_{\vec{k}'}$  is the weight associated to the special point  $\vec{k}'$  in the IBZ. By following this method, 10 special  $\vec{k}$  points in the IBZ are sufficient to get converged  $\Sigma^{\text{sex}}$  within few tens of meV.

Because of the presence of the static screened exchange term, each GW correction to a given  $E_{n\vec{k}'}^{(0)}$  scales as  $N_{\vec{k}} N N_{\text{PW}}$ , where  $N_{\vec{k}}$ ,  $N$  and  $N_{\text{PW}}$  are the number of  $\vec{k}$  points used in the summation of the charge, of occupied electronic states, and of the plane waves used in the expansion of the Kohn–Sham orbitals, respectively.

### IV. MAGNESIUM OXIDE

The ground state properties obtained for the  $O_h^5$  phase (rocksalt) of magnesium oxide are summarized in Tab.II. They are computed by fitting the curve of total energy versus lattice parameter to the equation of state proposed by Murnaghan. One can note that our results compare well to other all-electron LDA calculations<sup>15,37</sup> and show slight discrepancies with respect to experimental data: the computed lattice parameter is underestimated by about 2% and the cohesive energy is about 15 % too large. We attribute these errors mainly to the use of the LDA.

The bandstructures, both in the LDA and including quasiparticle corrections, are shown in Fig.1 along high-symmetry lines in the BZ. In the following, we refer to the energy levels relative to the top of the valence band in the LDA calculation, which is arbitrarily set to zero. The bands are calculated at the theoretical equilibrium lattice parameter  $a_{\text{th}}=4.125$  Å. In Table III we detail the energy differences between electronic states at high-symmetry points in the BZ, computed either at the theoretical equilibrium lattice parameter  $a_{\text{th}}=4.125$  Å or at the experimental

one  $a_{\text{exp}}=4.211$  Å. One can easily see that some of the direct transitions, and in particular those at  $\Gamma$ , strongly depend upon the value of the lattice parameter. This is true at the LDA level, while the GW corrections are less sensitive to the actual value of  $a$ . In ionic rocksalt compounds, the value of the fundamental gap at the  $\Gamma$  point is indeed driven by the strong Madelung potential, which varies as the inverse of the lattice parameter.

In agreement with a previous full GW calculation<sup>15</sup>, the quasiparticle corrections consist of a rigid shift of the conduction band (CB) with respect to the valence band (VB) — that is, application of a scissor operator, which is modulated by smooth  $\vec{k}$  dependent terms of the order of 10 % of the rigid shift itself. The total valence bandwidth  $\Gamma_{15,v} - \Gamma_{1,v}$  changes from 17.3 eV in LDA to 20.1 eV with quasiparticle corrections. Similarly, the  $L'$  and  $X_1$  points move  $\simeq 2$  eV downwards from the the valence band maximum (VBM), as one can see from Fig.1. This improves the accordance with the experimental XPS spectra which show a main peak at 18 eV and a shoulder at 21 eV below the VBM<sup>38</sup>. The fundamental band gap passes from 5.21 eV to 8.88 eV.

In all these calculations, we assume the experimental value  $\epsilon_{\infty} = 2.95$ <sup>39</sup> for the static dielectric constant. Recently, through an *ab initio* calculation of the dielectric function within the LDA, Shirley found  $\epsilon_{\infty} = 3.03$ , at the experimental lattice parameter<sup>40</sup>. In order to test the sensitivity of our theoretical scheme to the choice of  $\epsilon_{\infty}$ , which enters as a parameter in our model screening function defined in Eq.6, we performed an additional GW calculation by adopting  $\epsilon_{\infty} = 3.50$ . Consistently with a stronger screening, the direct transition energies at high-symmetry points are lowered by  $\simeq 0.5$  eV at most.

It is interesting to note that the main corrections to the Kohn-Sham eigenvalues of VB states come from the static screened exchange term  $\Sigma^{\text{sex}}$  (Eq.8), while the coulomb hole contribution  $\Sigma^{\text{coh}}$  dominates the quasiparticle corrections to the eigenvalues of the CB. For instance,  $\Sigma_{\Gamma_1}^{\text{sex}} \simeq -16$  eV and  $\Sigma_{\Gamma_1}^{\text{coh}} \simeq -10$  eV at the bottom of the VB, while  $\Sigma_{\Gamma_1}^{\text{sex}} \simeq -5$  eV and  $\Sigma_{\Gamma_1}^{\text{coh}} \simeq -8$  eV at the bottom of the CB. This is consistent with the more localized nature of the VB states with respect to the CB states. The same remark applies to SrO and SrTiO<sub>3</sub>, which are discussed in the following sections.

As far as the interpretation of the main optical transitions is concerned, we indicate in Table III the experimental values with their tentative assignement, according to Schömberger and Aryasetiawan<sup>15</sup>. We agree with their interpretation, since our GW values, computed at the experimental lattice constant, differ by  $\simeq 1$  eV at most from theirs. Our calculations slightly overestimate the experimental transition energies.

MgO	$a$ (Å)	$B$ (Mbar)	$E_{\text{coh}}$ (eV)
Experiment	4.211	1.55 <sup>41</sup>	10.33
Ref. 42	4.191	1.46	
Ref. 15	4.16		
Ref. 37	4.09	1.71	10.67
Present work	4.125	1.56	11.80

TABLE II. Structural properties of Cubic MgO. A comparison is made with other LDA calculations, in a pseudopotential approach<sup>42</sup> or using LMTO<sup>15,37</sup>

MgO	$E_g(\Gamma)$	$E_g(X)$	$E_g(L)$	Minimal Gap
Experiment <sup>43</sup>	7.7	13.3	10.8	7.7 ( $\Gamma - \Gamma$ )
HF+pol. <sup>44</sup>	8.21	15.79	11.48	8.21 ( $\Gamma - \Gamma$ )
LDA <sup>15</sup>	5.2	10.5	8.9	5.2 ( $\Gamma - \Gamma$ )
LDA+GW <sup>15</sup>	7.7	13	11.4	7.7 ( $\Gamma - \Gamma$ )
LDA <sup>40</sup>	4.73			4.73 ( $\Gamma - \Gamma$ )
LDA+GW <sup>40</sup>	7.81			7.81 ( $\Gamma - \Gamma$ )
this work				
LDA <sup>†</sup>	5.21	10.40	8.93	5.21 ( $\Gamma - \Gamma$ )
LDA <sup>‡</sup>	4.61	10.26	8.46	4.61 ( $\Gamma - \Gamma$ )
LDA+GW <sup>†</sup>	8.88	14.43	12.99	8.88 ( $\Gamma - \Gamma$ )
LDA+GW <sup>‡</sup>	8.20	14.22	12.46	8.20 ( $\Gamma - \Gamma$ )

TABLE III. Direct gaps of Cubic MgO (in eV). Our results are given both in the LDA and with quasiparticle corrections (LDA+GW), either at the theoretical equilibrium lattice constant (<sup>†</sup>) or at the experimental one (<sup>‡</sup>). The theoretical calculations of Refs. 44,15,40 are all carried out at the experimental lattice constant.

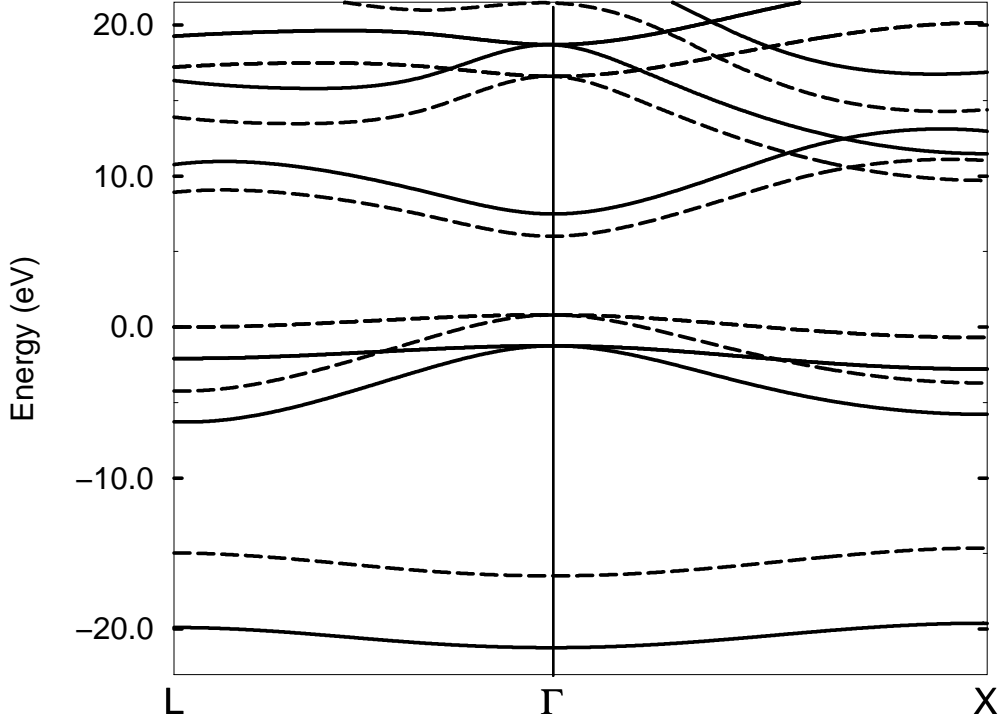


FIG. 1. Computed bands of cubic MgO at the theoretical lattice parameter. Solid lines: GW bands. Dashed lines: LDA bands. The top of the LDA valence bands is arbitrarily set to zero.

## V. STRONTIUM OXIDE

The ground state properties computed for the  $O_h^5$  phase of SrO are summarized in Tab.IV. The bandstructures, computed in LDA and with QP corrections, are shown in Fig.2 along high symmetry directions.

A deep band, originating mainly from Sr 4s states, is not shown in the figure. It is found around -30.5 eV in the LDA calculation, with a dispersion less than 1eV. The QP corrections shift this band to lower energies, about 33 eV below the valence band maximum (VBM).

The bands of lowest energy shown in Fig.2 originate from Sr 4p and O 2s states. In the LDA, the bandwidth is about 4.3 eV, while the GW corrections push that band towards higher binding energies, and split it in two less dispersive structures, of which the lower originates from O 2s states mainly, and the upper from Sr 4p states. The splitting between O 2s and Sr 4p levels is essentially due to the larger  $\Sigma^{\text{sex}}$  contribution for the former states, as a consequence of their stronger localization.

As far as the deep VB levels are concerned, XPS experiments<sup>38</sup> found two broad peaks at  $\simeq -35$  eV (*A*) and  $\simeq -17.5$  eV (*B*) below the top of the valence band. The authors assigned the *A* structure to the band arising from Sr 4s states, and the *B* structure to those coming from O 2s and Sr 4p states. The resolution, however, was too poor for them to resolve the two latter contributions to peak *B*. The positions of the deep VB levels are badly accounted for in the LDA, which would yield the *A* peak at -30.5 eV and a broader *B* structure around -13 eV. On the other hand, Hartree-Fock calculations including correlation<sup>44</sup> give a separation of about 6.5 eV between the O 2s and the Sr 4p states, which is likely overestimated. A better agreement with experimental data is obtained through the inclusion of GW corrections, which shift the Sr 4s band to  $\simeq -33$  eV and give two contributions to the electronic density of states at  $\simeq -18$  eV and  $\simeq -14$  eV with respect to the VBM, about 0.5 eV wide. The latters seem consistent with the broad *B* structure seen in XPS<sup>38</sup>. A later XPS investigation<sup>45</sup> found a splitting  $\Delta_{AB}$  between the *A* and the *B* structure equal to 17.9 eV, which was interpreted as the difference in the binding energy of Sr 4s and 4p levels in SrO. Since it seems difficult to disentangle the Sr 4p and the O 2s contribution to the *B* structure, we compare the minimum and the maximum splitting  $\Delta_{AB}$  as obtained in our calculations. In the LDA,  $\Delta_{AB}$  ranges from 14.5 eV to 17.5 eV, while that obtained by including the GW corrections ranges from 16 eV to 19 eV and better agrees with the XPS data.

The upper part of the valence band results very similar in the LDA and GW calculations. Its width is 2.2 eV in LDA and 2.1 eV after GW corrections. The dispersions of both QP and LDA eigenvalues along high-symmetry directions are very similar, too.

The lower part of the conduction band drawn in the figures is shifted upward by GW corrections, opening the LDA gap by about 3 eV, with additional and small corrections depending on the particular band and  $\vec{k}$  point as one can see in Table (V). In particular, the direct gap at  $\Gamma$  ( $X$ ) passes from  $E_g(\Gamma) = 4.29$  eV ( $E_g(X) = 3.03$  eV) in LDA to  $E_g(\Gamma) = 7.54$  eV ( $E_g(X) = 6.39$  eV) after GW corrections. It is important to note that the direct gap  $\Gamma_{15} - \Gamma_1$  is strongly sensitive to the precise value of the lattice parameter  $a_0$ : while the above value  $E_g(\Gamma) = 4.29$  eV is calculated at the LDA equilibrium lattice parameter  $a_{\text{th}}$ , at  $a_{\text{exp}} = 5.16\text{\AA}$  we find a smaller  $E_g(\Gamma) = 3.92$  eV, *i.e.* a reduction of about 0.4 eV. The behaviour at the  $X$  point is different, since the  $E_g(X)$  calculated at  $a_{\text{exp}}$  is equal to 3.11 eV, about 0.1 eV bigger than that computed at  $a_{\text{th}}$ . Given the different nature of the electronic states at the various symmetry points in the BZ, a non trivial dependence of the eigenvalues upon the structural parameters is generally expected<sup>46</sup>.

On the other hand, the QP energy differences obtained by our method are less dependent on the precise value of the optical dielectric constant used in the model screening (Eq.6). For instance,  $E_g(\Gamma)$  varies only by -3% when passing from  $\epsilon_{\infty} = 3.35$  to  $\epsilon_{\infty} = 3.7$ , which represents a 11% increase of the optical dielectric constant.

We are not aware of any angle-resolved photoemission or inverse photoemission experiments on SrO, able to provide direct experimental information on the band dispersion around the Fermi level. Thus, the comparison of our results to experimental data is mainly based on the information issued from reflectivity measurements. Rao and Kearney<sup>47</sup> conclude for direct gaps at  $\Gamma$  ( $X$ )  $E_g(\Gamma) = 5.9$  eV ( $E_g(X) = 6.28$  eV), and exciton binding energies at high-symmetry points of the BZ around 0.2 - 0.3 eV. Conversely, more recent optical measurements on well characterized single crystals of SrO<sup>48</sup> found  $E_g(X) = 5.79$  eV, lower than  $E_g(\Gamma) = 6.08$  eV. On the basis of the onset of the optical absorption spectra the authors also deduce that SrO has an indirect minimum gap, while BaO shows a direct gap at  $X$ . On the theoretical side, the nature of the fundamental gap of SrO is still debated: while both LMTO/LDA<sup>37</sup> and APW/X <sub>$\alpha$</sub> <sup>49</sup> calculations give an indirect gap  $\Gamma_{15} - X_3$  clearly underestimated (3.8 and 3.9 eV respectively), Pandey and coworkers<sup>44</sup> found a more realistic value  $E_g(\Gamma) = 7.11$  eV and  $E_g(X) = 9.11$  eV through a Hartree-Fock calculation including correlation at the second order in perturbation theory. These results confirm the general findings in other semiconducting and insulating materials, that DFT-LDA underestimates the fundamental gap, while the reverse happens in Hartree-Fock calculations, although the inclusion of correlations in the latters improves the agreement with experiments. Our GW corrected bands at the experimental lattice parameter, yield gaps at  $X$  and  $\Gamma$  equal to  $E_g(X) = 6.45$  eV and  $E_g(\Gamma) = 7.12$  eV respectively, presenting a better agreement with experimental data.

SrO	$a(\text{\AA})$	$B(\text{Mbar})$	$E_{\text{coh}}$ (eV)
Experiment	5.16	0.906	10.45
HF <sup>50</sup>	5.25	1.06	
LDA <sup>51</sup>	5.1-5.18	0.88-0.82	10.9-10.5
LDA <sup>37</sup>	5.22	1.07	9.59
Present work	5.07	1.04	11.9

TABLE IV. Structural properties of Cubic SrO. A comparison is made with Hartree-Fock (Ref. 50) and LDA calculations (Refs. 51,37).

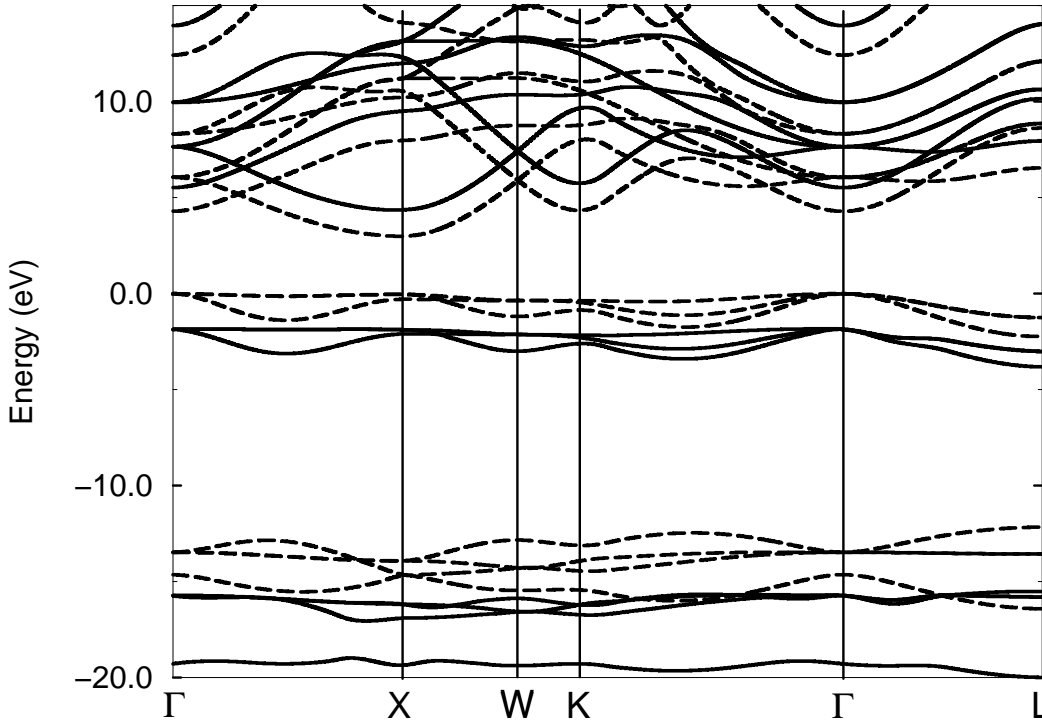


FIG. 2. Computed bands of cubic SrO, at the theoretical lattice parameter. Dashed line: LDA bands. Full line: GW bands. The zero is arbitrarily fixed at the top of the valence LDA band.

SrO	$E_g(\Gamma)$	$E_g(X)$	$E_g(L)$	Minimal Gap
Experiment				
Ref. 47	5.896	6.28		5.9 ( $\Gamma - \Gamma$ )
Ref. 48	6.08	5.79		
LDA (Ref. 37)	4.26			3.8( $\Gamma - X$ )
$X_\alpha$ (Ref. 49)	5.10	4.03	7.3	3.9( $\Gamma - X$ )
HF+corr. (Ref. 44)	7.11	9.11	12.36	8.54( $\Gamma - \Gamma$ )
Present work				
LDA <sup>†</sup>	4.29	3.03	7.79	3.00 ( $\Gamma - X$ )
LDA <sup>‡</sup>	3.92	3.11	7.47	3.04 ( $\Gamma - X$ )
LDA+GW <sup>†</sup>	7.54	6.39	11.17	6.37 ( $\Gamma - X$ )
LDA+GW <sup>‡</sup>	7.12	6.45	10.81	6.39 ( $\Gamma - X$ )

TABLE V. Gap of Cubic SrO (in eV), at the high-symmetry point of the Brillouin zone. The gaps are calculated either at the theoretical lattice parameter (<sup>†</sup>) or at the experimental one (<sup>‡</sup>).

## VI. STRONTIUM TITANATE

The computed ground-state properties of the cubic phase of  $\text{SrTiO}_3$ , such as the equilibrium lattice parameter, the bulk modulus and the cohesive energy, are showed in Table VI. A good agreement with previous LDA calculations<sup>52,53</sup> is found. We stress that in all these calculations the selfconsistent electron density includes the semicore states (Sr 4s, Sr 4p, Ti 3s and Ti 3p). With respect to experimental data, a slight underestimate (-1.3%) of the lattice parameter is obtained, while the computed cohesive energy is  $\simeq 20\%$  larger than that measured, as it is usual in the LDA. As far as the GW calculation is concerned, we adopt the experimental value  $\epsilon_\infty = 5.82$  of the optical dielectric constant of the cubic phase of  $\text{SrTiO}_3$ <sup>54</sup>. Both LDA and GW bands (Fig.3) are computed at the LDA theoretical equilibrium lattice parameter  $a_{\text{th}}$ .

Firstly, we discuss the positions of the deep lying states not shown in Fig.3. A deep, almost non dispersive, energy band is found at  $\simeq -54\text{eV}$  below the top of the valence band (VBM) in the LDA calculations, which originates from Ti 3s states. The inclusion of QP corrections in our GW scheme pushes it downward, at  $-58.9\text{ eV}$  below the VBM. This is in very good agreement with XPS measurements<sup>38</sup>, which show a peak around -59 eV.

Analogously, in the LDA calculation, the narrow bands originating mainly from Ti 3p states are located at  $-30.5\text{ eV}$  below VBM, very close to a band with dominant Sr 4s character, at about  $-29.5\text{ eV}$ . GW corrections push them at  $-33.7\text{ eV}$  and  $-32.7\text{ eV}$ , respectively. The XPS spectra show a 2 eV wide asymmetric peak centered at  $\simeq -34.5\text{ eV}$ <sup>38</sup>. As found for the Ti 3s band, the inclusion of quasiparticle effects greatly improves the agreement with the experimental data.

The very broad structure in the XPS data<sup>38</sup> between  $-20\text{ eV}$  and  $-14\text{ eV}$  originating from O 2s and Sr 4p states is fully consistent with the position of our GW bands, while the LDA bands are higher in energy by about 3 eV on average.

The valence band portion shown in Fig.3 has a dominant O 2p character with non negligible contributions from Ti 3d states, mainly in its lower part. It is less sensitive to GW corrections, which almost rigidly shift the bands towards lower energies. As a consequence, the LDA and GW bandwidths along the  $\Delta$  line ( $4.15\text{ eV}$  and  $4.11\text{ eV}$ , respectively) are both in very good agreement with the value of  $4.2\text{ eV}$  measured in angle-resolved photoemission<sup>6</sup>. Similarly, the total bandwidth  $R_{1,v} - R_{12,v}$  (see also Fig.3) turns out to be  $4.8\text{ eV}$  in the LDA and  $4.9\text{ eV}$  with quasiparticle corrections.

A major difference between the LDA and GW results regards the direct band gaps, which roughly differ by about 3 eV. The onset for optical absorption was measured at  $3.2\text{ eV}$  by Cardona<sup>55</sup> and at  $3.34\text{ eV}$  by Blazey<sup>56</sup>, and interpreted as a  $\Gamma_{15,v} \rightarrow \Gamma_{25',c}$  transition. The strong absorption peaks at  $\simeq 4 - 5\text{ eV}$  were attributed to vertical transitions at  $X$  and  $M$ , respectively. On the other hand, the fundamental gap derived from combined photoemission and inverse photoemission spectra, which is free from excitonic effects, was estimated to be  $(3.3 \pm 0.5)\text{ eV}$ <sup>57</sup>. With respect to these experimental values, the LDA  $E_g(\Gamma)$  is underestimated by almost 1 eV, while the GW one is overestimated by about 2 eV (see Table VI) In this respect, the inclusion of self-energy corrections at a perturbative level does not improve the LDA. This issue is discussed in the next section, in relation to the validity of our model screening for transition metal oxides such as  $\text{SrTiO}_3$ .

$\text{SrTiO}_3$	$a(\text{\AA})$	$B(\text{Mbar})$	$E_{\text{coh}}(\text{eV})$
Experiment	3.903	1.83	31.7
Ref. 52	3.870	1.94	
Ref. 53	3.864	1.99	
This work	3.850	2.03	37.88

TABLE VI. Structural properties of cubic  $\text{SrTiO}_3$ . Both Refs. 52,53 use the LDA with ultra-soft pseudopotentials. The experimental values of  $a$  and  $E_{\text{coh}}$  are quoted in Ref. 58 and  $B$  is taken from Ref. 59.

SrTiO <sub>3</sub>	$E_g(\Gamma)$	$E_g(X)$	$E_g(M)$	$E_g(R)$	Minimal Gap
LDA <sup>52</sup>	2.16				1.79 ( $R-\Gamma$ )
LDA <sup>60</sup>	3.77	4.1		5.2	2.88 ( $R-\Gamma$ )
This work					
LDA	2.24	2.85	4.17	4.82	1.90 ( $R-\Gamma$ )
LDA+GW	5.42	6.10	7.29	8.15	5.07 ( $R-\Gamma$ )

TABLE VII. Computed  $E_g$  for direct transitions from the VB to the CB of cubic SrTiO<sub>3</sub>, in eV. The minimal gap is also given.

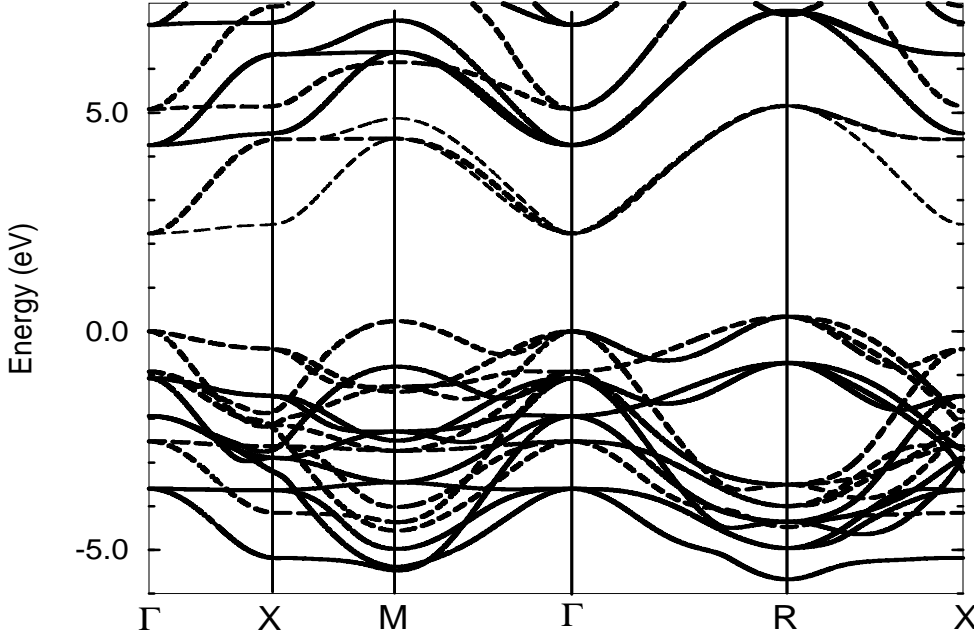


FIG. 3. Upper part of the valence bands and lower part of the conduction bands of cubic SrTiO<sub>3</sub>, at the theoretical equilibrium lattice parameter. Dashed lines: LDA bands. Solid line: GW bands.

## VII. DISCUSSION

The agreement of our numerical results with the available experimental data is rather inhomogeneous: while for MgO and SrO a reasonable agreement is found, for SrTiO<sub>3</sub> the QP bands around the Fermi level seem to be worse than the LDA ones. It is the aim of this section to discuss our results with respect to two points: On the one hand, the quality of the ground-state calculation from which the perturbative GW calculation starts. On the other hand, the reliability of our model dielectric function used in the calculation of the QP spectra of the oxides considered here.

We have found that the values of the direct gaps are very sensitive to the value of the lattice parameter. A good description of the ground state structural properties is thus a prerequisite to obtain QP spectra that can be compared to experimental data reliably. This is especially the case of MgO and SrO. In Table VIII the relative variations  $\Delta_g(\vec{k})$  of the direct gaps, both in the LDA and in the GW approximation, are given as a function of the lattice parameter. One can note that: (i) The largest variations of the direct gaps  $\Delta_g(\vec{k})$  are nearly always obtained at the LDA level. (ii)  $\Delta_g(\vec{k})$  depends on the actual  $\vec{k}$  point, consistently with the character of the wavefunction. The largest  $\Delta_g(\vec{k})$  are generally found for the strongest bonding-antibonding combinations across the gap. (iii) Increasing  $\Delta_g(\Gamma)$  are found for SrTiO<sub>3</sub>, SrO and MgO, in ascending order.

One should thus be careful when discussing the quality of the self-energy corrections to the electronic structure, since it may be strongly dependent on variables, such as the lattice parameter, which are *external* to the theory itself. Our data for MgO, obtained at the experimental lattice constants  $a_{\text{exp}}$ , compare well with other more sophisticated, *ab initio* GW results also using  $a_{\text{exp}}$ <sup>15,40</sup>, as far as the direct gaps are concerned (see Table III). Both for MgO and SrO, a fair accordance with experimental data is found when adopting  $a_{\text{exp}}$ . We thus conclude that, still at the level of the ground state structural properties, one should obtain a good agreement with experimental data (for example, by using generalized gradient corrections to the LDA) before starting the calculation of the quasiparticle energies.

Care must also be taken when comparing the theoretical gaps and those derived from optical measurements, because of the existence of excitonic effects in the latters, not accounted for in the present theory. For MgO, these effects should be rather small, as suggested experimentally by Roessler and Walker<sup>43</sup> and calculated by Benedict and coworkers<sup>62</sup>. For SrO and SrTiO<sub>3</sub> there is still a lack of *ab initio* calculations of one- and two-particle excitations to address fully this issue.

Another important point is the quality of the quasiparticle corrections, in relation to the model dielectric function  $\epsilon(q, \tilde{\rho})$  used in the GW calculation. As it is evidenced by Eq.6, the screening depends on the value of the optical

dielectric constant  $\epsilon_\infty$  of the oxide. As in the previous discussions regarding the lattice parameter, one can use either the experimental optical dielectric constant available in the literature, or compute it in the framework of the self-consistent theory adopted, such as the DFT. In a recent paper, Shirley<sup>40</sup> obtained for MgO a theoretical optical dielectric constant, at the *experimental* lattice parameter,  $\epsilon_\infty^{(\text{th})} = 3.03$  in the LDA, to be compared with the measured  $\epsilon_\infty = 2.95$ <sup>39</sup>. Extrapolating our results – obtained with  $\epsilon_\infty = 2.95$  and  $\epsilon_\infty = 3.50$  (see Sec.IV) – we can conclude that our quasiparticle energies would vary by less than 0.1 eV when passing from  $\epsilon_\infty = 2.95$  to  $\epsilon_\infty^{(\text{th})} = 3.03$ . However, a more satisfactory theoretical framework would be to compute  $\epsilon_\infty$  from first principles, in conjunction with the use of an approximation for the exchange–correlation energy, capable to reproduce the experimental lattice constant. Although in the present case the results would not be much affected, this would open the way to the calculation of quasiparticle excitations of systems for which no experimental measurements of the optical dielectric constant are available. On the other hand, the use of model dielectric functions might open the possibility to treat complex systems consisting of many inequivalent atoms, such as low-symmetry crystals, surfaces and heterostructures.

Considering the numerical results obtained, and the previous discussion, we note that the model dielectric function works reasonably well for both MgO and SrO, which are compounds with fundamental gaps much larger than the semiconductors ZnSe, GaN, and SiC previously studied with the same method<sup>21,23</sup>. We thus conclude that the validity of the screening model (Eq.6) is neither a function of the gap value nor of the ionocovalent character of the bonding in the crystal under study. On the other hand, it fails when applied to SrTiO<sub>3</sub>, a transition metal oxide characterized by a moderate optical gap (slightly larger than 3 eV according to Refs. 6,56).

In order to clarify the reasons for such a failure, we computed the bare exchange contribution to the QP gap at the  $\Gamma$  point, for both MgO (10.46 eV) and SrTiO<sub>3</sub> (12.28 eV), in first-order perturbation theory. This difference stems from the different character of the states at the bottom of the conduction bands, which have a Ti 3d character in the case of SrTiO<sub>3</sub>, and are much flatter than those of MgO, having a dominant Mg 3s character. This is fully consistent with the stronger localization of the Ti 3d states, which could make our treatment of local-field effects (see Eqs.6 and 7) rather inappropriate. In fact, the choice of the effective density  $\tilde{\rho}_{n\vec{k}}$  (Eq.8) takes into account the different localization of the states only through their superposition with the electron density  $\rho(\vec{r})$ . Moreover, its definition contains an ambiguity, since its precise value depends on the core–valence partitioning of  $\rho(\vec{r})$ . It is interesting to consider the extreme limit in which  $\epsilon(q, \tilde{\rho})$  is no longer  $q$  dependent and is simply replaced by the optical dielectric constant  $\epsilon_\infty$ . In this limit of screening, the only contribution to the GW correction to the DFT–LDA gap comes from the screened–exchange term, since the Coulomb hole gives a rigid shift equal for all the bands. Interestingly, this correction provides gap values equal to 4.3 eV for MgO and 2.7 eV for SrTiO<sub>3</sub>, in much better agreement with experiments in the latter case than when using  $\epsilon(q, \tilde{\rho}_{n\vec{k}})$  given by Eq.6. This points out the need for a better inclusion of local field effects in the model dielectric function for transition metal oxides, such as SrTiO<sub>3</sub>. Another source of failure relatively to SrTiO<sub>3</sub> could be also the use of a perturbative GW scheme: a possible solution to this issue would be the use of an efficient self-consistent GW approach which has shown to give good results even in systems in which  $d$  orbitals play a fundamental role<sup>63</sup>.

	MgO	SrO	SrTiO <sub>3</sub>
$(a_{\text{th}} - a_{\text{exp}})/a_{\text{exp}}(\%)$	-2.0	-1.7	-1.3
$\Delta_g^{\text{LDA}}(\Gamma)$	-6.4	-5.4	-1.7
$\Delta_g^{\text{GW}}(\Gamma)$	-4.1	-3.6	
$\Delta_g^{\text{LDA}}(X)$	-0.7	1.5	-2.2
$\Delta_g^{\text{GW}}(X)$	-0.7	0.6	
$\Delta_g^{\text{LDA}}(L)$	-2.7	-2.5	-4.4
$\Delta_g^{\text{GW}}(L)$	-2.1	-2.0	

TABLE VIII. Dependence of the direct gaps  $E_g(\vec{k})$  of MgO, SrO and SrTiO<sub>3</sub> at high-symmetry points  $\vec{k}$  of the Brillouin zone as a function of the relative variations of the lattice parameter  $(a_{\text{th}} - a_{\text{exp}})/a_{\text{exp}}$ . The function  $\Delta_g$  is defined as  $\frac{E_g(a_{\text{th}}) - E_g(a_{\text{exp}})}{E_g(a_{\text{exp}})} \frac{a_{\text{exp}}}{a_{\text{th}} - a_{\text{exp}}}$ . The values are computed either by using the LDA, or by including quasiparticle corrections within the GW approximation.

## VIII. CONCLUSIONS

We have calculated the ground state properties of cubic oxides  $\text{MgO}$ ,  $\text{SrO}$  and  $\text{SrTiO}_3$  within the DFT-LDA, and applied a perturbative GW method, based on a dielectric model which includes approximately local field and dynamical effects, to determine their quasiparticle energies. We have tested the dependence of the calculated spectra on the parameters entering the calculation, such as the optical dielectric constant  $\epsilon_\infty$  and the lattice parameter  $a$ . In particular, we have shown that quasiparticle energies in alkaline-earth oxides are sensitive functions of the lattice parameter, even at the LDA level. As a consequence, the use of either the experimental or the theoretical values for  $a$  can influence the quality of the results whenever  $a_{\text{th}}$  differs from  $a_{\text{exp}}$ .

Through a careful comparison with the available experimental data and previous ab-initio GW calculations, we have shown that the simplified GW method works reasonably well for systems, such as  $\text{MgO}$  and  $\text{SrO}$ , in which the electronic states of the valence band and the bottom of the conduction band mainly consist of  $s$ - and  $p$ -like states. Moreover, in the three oxides, GW corrections have been found to be crucial to account for the energies of semicore electron states, such as  $\text{O } 2s$ ,  $\text{Ti } 3s$ ,  $\text{Ti } 3p$ ,  $\text{Sr } 4s$  and  $\text{Sr } 4p$ , which agree well with the peak positions recorded in photoemission spectra. When localized  $d$ -like states contribute to bands around the Fermi level, our method produces an overestimation of the self-energy corrections. This is the case of  $\text{SrTiO}_3$ , for which it is not clear at this stage whether a higher order perturbative approach, in which the LDA wavefunctions are renormalized, is needed, or whether this failure calls for a more refined treatment of local-field effects.

We thank Lucia Reining for fruitful discussions and careful reading of the manuscript, Tristan Albaret for his help in generating the pseudopotentials, and Eric Shirley for kindly providing us unpublished results on self-energy corrections for  $\text{MgO}$ . Computing resources were granted by the IDRIS/CNRS computational centre in Orsay, under project 980864. G.C. acknowledges support from the Commission of the European Communities (framework IV) programme under the Networks scheme.

- <sup>1</sup> C. Noguera, *Physics and chemistry of oxide surfaces*, Cambridge University Press (1996).
- <sup>2</sup> F. Bechstedt, Adv. Solid State Phys. **32**, 161 (1992).
- <sup>3</sup> C. Noguera and W.C. Mackrodt, J. Phys. Cond. Matt. **12**, 2163 (2000).
- <sup>4</sup> W.C. Mackrodt, N.M. Harrison, V.R. Saunders, N.L. Allan, M.D. Towler, Chem. Phys. Lett. **250**, 66 (1996).
- <sup>5</sup> L.H. Tjeng, A.R. Vos and G.A. Sawatzky, Surf. Sci. **235**, 269 (1990).
- <sup>6</sup> N. B. Brookes, D. S.-L. Law, T. S. Padmore, D. R. Waeburton and G. Thornton, Solid State Comm. **57**, 473 (1988).
- <sup>7</sup> G.N. Raikar, P.J. Hardman, C. A. Muryn, G. van der Laan, P.L. Wincott, G. Thornton and D.W. Bullett, Solid State Comm. **80**, 423 (1991).
- <sup>8</sup> P.J. Hardman, P.L. Wincott, G. Thornton, D.W. Bullett and P.A.D.M.A. Dale, Phys. Rev. B **49**, 7170 (1994).
- <sup>9</sup> L. Hedin, Phys. Rev. **139**, A796 (1965); L. Hedin and S. Lundqvist, Solid State Phys. **23**, 1 (1969).
- <sup>10</sup> M.S. Hybertsen and S.G. Louie, Phys. Rev. B **34**, 5390 (1986).
- <sup>11</sup> R. Godby, M. Schlüter and L. J. Sham, Phys. Rev. B **37**, 10159 (1988).
- <sup>12</sup> M. Röhlfing, P. Krüger and J. Pollmann, Phys. Rev. B **57**, 6485 (1998).
- <sup>13</sup> E.L. Shirley, Phys. Rev. Lett. **80**, 794 (1998).
- <sup>14</sup> B. Králik, E.K. Chang and S.G. Louie, Phys. Rev. B **57**, 7027 (1998).
- <sup>15</sup> U. Schömberger and F. Aryasetiawan, Phys. Rev. B **52**, 8788 (1995).
- <sup>16</sup> O. Pulci, G. Onida, R. Del Sole and L. Reining, Phys. Rev. Lett. **81**, 5347 (1998).
- <sup>17</sup> M. Röhlfing, S.G. Louie, Phys. Rev. Lett. **83**, 856 (1999).
- <sup>18</sup> F. Bechstedt, R. Del Sole, Phys. Rev. B **38**, 7710 (1988).
- <sup>19</sup> F. Gygi, A. Baldereschi, Phys. Rev. Lett. **62**, 2160 (1989).
- <sup>20</sup> F. Bechstedt, R. Del Sole, G. Cappellini, L. Reining, Solid State Comm. **84**, 765 (1992).
- <sup>21</sup> M. Palummo, R. Del Sole, L. Reining, F. Bechstedt, G. Cappellini, Solid State Comm. **95**, 393 (1995).
- <sup>22</sup> G. Cappellini, V. Fiorentini, K. Tønnesen and F. Bechstedt, Mat. Res. Soc. Symp. Proc. **395**, 429 (1996).
- <sup>23</sup> B. Wenzien, G. Cappellini, F. Bechstedt, Phys. Rev. B **51**, 14701 (1995).
- <sup>24</sup> B. Wenzien, P. Käckell, F. Bechstedt, G. Cappellini, Phys. Rev. B **52**, 10897 (1995).
- <sup>25</sup> P. Fulde, *Electron Correlations in Molecules and Solids*, Springer-Verlag, Berlin (1991).
- <sup>26</sup> W. Kohn and L. J. Sham, Phys. Rev. **140**, A1133 (1965).
- <sup>27</sup> M.S. Hybertsen and S.G. Louie, Phys. Rev. B **37**, 2733 (1988).
- <sup>28</sup> L. Reining, G. Onida, R. W. Godby, Phys. Rev. B **56**, 4301 (1997).

<sup>29</sup> Z.H. Levine, S.G. Louie, Phys. Rev. B **25**, 6310 (1982).

<sup>30</sup> G. Cappellini, R. Del Sole, L. Reining, F. Bechstedt, Phys. Rev. B **47**, 9892 (1993).

<sup>31</sup> D. M. Ceperley and B. J. Alder, Phys. Rev. Lett. **45**, 566 (1980).

<sup>32</sup> X. Gonze, R. Stumpf and M. Scheffler, Phys. Rev. B **44**, 8503 (1991).

<sup>33</sup> N. Troullier and J. L. Martins, Phys. Rev. B **43**, 1993 (1991).

<sup>34</sup> H.J. Monkhorst and J.D. Pack, Phys. Rev. B **13**, 5188 (1976).

<sup>35</sup> We used both a Cray C90 computer and a Digital  $\alpha$ -500 workstation, with 512 MB of memory.

<sup>36</sup> F. Gygi, A. Baldereschi, Phys. Rev. B **34**, 4405 (1986).

<sup>37</sup> O. E. Taurian, M. Springborg and N. E. Christensen, Solid State Comm. **55**, 351 (1985).

<sup>38</sup> S.P. Kowalczyk, F.R. McFeely, L. Ley, V.T. Gritsyna and D.A. Shirley, Solid State Comm. **23**, 161 (1977).

<sup>39</sup> R.C. Whited, C.J. Flaten and W.C. Walker, Solid State Comm. **13**, 1903 (1973).

<sup>40</sup> E. Shirley, Phys. Rev. B **58**, 9579 (1998).

<sup>41</sup> M. J. L. Sangster, G. Peckam, and D. H. Saunderson, J. Phys. C **3**, 1026 (1970).

<sup>42</sup> K. J. Chang and M. L. Cohen, Phys. Rev. B **30**, 4774 (1984).

<sup>43</sup> D.M. Roessler and W.C. Walker, Phys. Rev **159**, 733 (1967).

<sup>44</sup> R. Pandey, J. E. Jaffe, and A. B. Kunz, Phys. Rev. B **43**, 9228 (1991).

<sup>45</sup> H. van Doveren and J. A. Th. Verhoeven, J. Electr. Spectr. Rel. Phenom. **21**, 265 (1980).

<sup>46</sup> In SrO, the bottom of the conduction band  $X_{3,c}$  has mainly Sr 4d character, while at  $\Gamma_{1,c}$  the Sr 5s character prevails. In any case, a noticeable degree of second-neighbour hybridization is present.

<sup>47</sup> A. S. Rao and R. J. Kearney, Phys. Stat. Sol. (b) **95**, 243 (1979).

<sup>48</sup> Y. Kaneko and T. Koda, J. Cryst. Growth **86**, 72 (1988).

<sup>49</sup> A. Hasegawa and A. Yanase, J. Phys. C **13**, 1995 (1980).

<sup>50</sup> A. Zupan, I. Petek, M. Causà and R. Dovesi, Phys. Rev. B **48**, 799 (1993).

<sup>51</sup> P. Cortona and A. Villaflorita Monteleone, J. Phys. Cond. Matt. **8**, 8983 (1996).

<sup>52</sup> S. Kimura, J. Yamauchi, M. Tsukada and S. Watanabe, Phys. Rev. B **51**, 11049 (1995).

<sup>53</sup> R.D. King-Smith and D. Vanderbilt, Phys. Rev. B **49**, 5828 (1994).

<sup>54</sup> P. Dore, A. Paolone and R. Trippetti, J. Appl. Phys. **80**, 5271 (1996).

<sup>55</sup> M. Cardona, Phys. Rev. **140**, A 651 (1965).

<sup>56</sup> K.W. Blazey, Phys. Rev. Lett. **27**, 146 (1971).

<sup>57</sup> Y. Tezuka, S. Shin, T. Ishii, T. Ejima, S. Suzuki and S. Sato, J. Phys. Soc. Japan **63**, 347 (1994)

<sup>58</sup> K.H. Weyrich and R. Siems, Z. Phys. B **61**, 63 (1985).

<sup>59</sup> G.J. Fischer, Z. Wang and S.-I. Karato, Phys. Chem. Miner. **20**, 97 (1993).

<sup>60</sup> Y. N. Xu and W. Y. Ching, Phys. Rev. B **44**, 7787 (1991).

<sup>61</sup> E. Shirley, private communication (1999)

<sup>62</sup> L.X. Benedict, E.L. Shirley and R.B. Bohn, Phys. Rev. Lett. **80**, 4514, (1998).

<sup>63</sup> S. Massidda, A. Continenza, M. Posternak and A. Baldereschi, Phys. Rev. B **55**, 13494 (1997).